# A system for the high-throughput analysis of acute thermal avoidance and adaptation in *C. elegans*

Andrei-Stefan Lia, Dominique A. Glauser*

Department of Biology, University of Fribourg, Fribourg, Switzerland

*Corresponding author: Dominique A. Glauser, Email: dominique.glauser@unifr.ch

Competing interests: The authors have declared that no competing interests exist.

## ABSTRACT

Nociception and its plasticity are essential biological processes controlling adaptive behavioral responses in animals. These processes are also linked to different pain conditions in human and have received considerable attention, notably *via* studies in rodent models and the use of heat-evoked withdrawal behavior assays as a readout of unpleasant experience. More recently, invertebrates have also emerged as useful complementary models, with their own set of advantages, including their amenability to genetic manipulations, the accessibility and relative simplicity of their nervous system and ethical concerns linked to animal suffering. Like humans, the nematode *Caenorhabditis elegans* (*C. elegans*) can detect noxious heat and produce avoidance responses such as reversals. Here, we present a methodology suitable for the high-throughput analysis of *C. elegans* heat-evoked reversals and the adaptation to repeated stimuli. We introduce two platforms: the INFERNO (for infrared-evoked reversal analysis platform), allowing the quantification of the thermal sensitivity in a petri dish containing a large population (> 100 animals), and the ThermINATOR (for thermal adaptation multiplexed induction platform), allowing the mass-adaptation of up to 18 worm populations at the same time. We show that wild type animals progressively desensitize in response to repeated noxious heat pulses. Furthermore, analyzing the phenotype of mutant animals, we show that the mechanisms underlying baseline sensitivity and adaptation, respectively, are supported by genetically separable molecular pathways. In conclusion, the presented method enables the high-throughput evaluation of thermal avoidance in *C. elegans* and will contribute to accelerate studies in the field with this invertebrate model.

**Keywords:** computer-assisted behavioral analysis, nematode, noxious heat avoidance, sensory plasticity, worm

## INTRODUCTION

Animal survival depends on the ability to efficiently avoid threats and damages. Nociception, the sensation of noxious stimuli, is therefore a widespread mechanism found throughout the animal kingdom. The molecular and cellular mechanisms involved are also widely conserved [1,2]. In human, nociceptive pathways serve as a primary trigger for innate acute withdrawal reflexes, for nociceptive pain perception, and are also involved in some chronic pain conditions. As such, nociceptive processes and their plasticity have received considerable attention, in the hope to improve therapeutic approaches in pain management [3]. Various animal models, mostly rodents, have been used to investigate this question [4]. Since animals cannot verbally report the intensity of unpleasant feeling, several pain assays were developed in order to

indirectly detect nociceptive responses and/or pain-like states. Among them, reflexive pain assays involving the delivery of noxious heat stimuli and the recording of withdrawal response (flick test [5], hot-plate test [6,7] and Hargreaves' method [8]) have been extensively used.

Several aspects limit research with mammalian pain models, however. One of them regards the ethical concerns linked to the induction of animal suffering. Another set of difficulties relate to the intrinsic complexity of the mammalian nervous system in general, and of the nociceptive molecular and cellular pathways in particular. For instance, the primary nociceptive neurons constitute an extremely heterogeneous population of sensory neurons [9,10], further intermingled with numerous non-nociceptive somatosensory neurons, and are not straightforward to identify and access. Circumventing these limitations, fruitful research using invertebrates demonstrated that they may constitute useful com-

plementary models, in particular to identify and characterize under-lying molecular mechanisms [1,11-13]. Among them, the nematode *Caenorhabditis elegans* (*C. elegans*) model is particularly attractive and presents many remarkable features. First, its nervous system is compact (302 neurons) and its wiring diagram has been fully mapped [14]. Second, it is a potent genetic model, amenable to genome-wide genetic screens [15,16]. Third, it presents robust innate avoidance behavior in response to noxious stimuli, including heat [17]. Fourth, the molecular mechanisms involved in nociception present striking similarities with that of mammals. Hence, key molecular components are conserved, such as TRP channels [18], and nociceptive responses are altered by cannabinoids [19,20], as well as many known painkiller drugs, such as nonsteroidal anti-inflammatory drugs and opiates [21,22].

*C. elegans* cannot grow at temperatures above ~26°C and exposure to higher temperatures may cause sterility or death. When exposed to heat, worms produce innate aversive responses that are essential to minimize thermal damage [23,24]. Whole animal stimulations or head-focused stimulations trigger a reversal response during which an animal moves backward for a certain distance (up to about three body lengths for strong stimuli) [17]. Reversals are often followed by a reorientation maneuver, called an omega turn, before the animal resumes forward locomotion. In contrast, tail-focused stimuli produce an acceleration of forward locomotion [17], whereas midbody stimulation causes a probabilistic response that could either be reversal, acceleration or pausing [25]. Interestingly, heat-evoked reversals can be triggered by actually harmful temperatures (which we will define here as > 26°C), but also in response to acute thermal stimuli that do not reach this harmful range, provided that the slope of the temporal temperature change is steep enough [26]. This nocifensive reversal response can thus be triggered by stimuli indicative of a potential danger before significant damages are produced. This situation is reminiscent of other nociceptive responses and seems particularly important in a tiny ectotherm whose temperature almost instantly equilibrates with that of in its surroundings.

Another interesting aspect of *C. elegans* thermal avoidance is its plasticity. Indeed, when pre-exposed to moderately noxious temperature for one hour, animals elevate their threshold for noxious heat avoidance. This plasticity involves the $Ca^{2+}$ signaling within thermosensory neurons and notably requires the $Ca^{2+}$/calmodulin-dependent protein kinase-1 (CMK-1) and its upstream regulatory kinase $Ca^{2+}$/calmodulin-dependent protein kinase kinase-1 (CKK-1) [27,28]. This pathway is also implicated in the response adaptation to other types of stimuli, such as adaptation in the innocuous range of temperature [29], salt learning [30], and habituation to repeated acute mechanical stimuli [31]. Nothing is known on whether animals would adapt in response to long-term, repeated noxious heat stimulations.

A variety of methods have been developed to stimulate *C. elegans* with noxious heat while the animal is crawling at the surface of an agar plate. A first approach is to use a heated metal probe (typically the tip of a soldering iron) brought at the vicinity of the worm [17]. This method is easy to implement, but the magnitude of the delivered stimulus is of limited precision and it is a relatively low-throughput approach, since a single worm is scored at a time. A second approach is to use a focused infrared light beam [25]. This approach enables the delivery of reliable and adjustable thermal stimuli, and can even be used to hit narrow regions along the animal body. Coupled with video recording and computer-assisted analysis, this approach can further

provide high-content phenotypic data. Its main drawbacks are that the system setup requires relatively advanced technical skills and that it is also relatively low-throughput, with single animals analyzed at a time. A third set of approaches involves population-based assays in which a specific spatial thermal pattern is created at the top of an agar plate and worm behavior is assessed by scoring the worm distribution after a certain time. These assays include (1) thermal barrier assays [18], in which one scores the fraction of animals able to crawl under a heated metal tube creating a sharp thermal barrier, (2) noxious heat thermogradient assays [18], in which one scores the distribution of animals along a spatial thermal gradient spanning over noxious temperatures and created with an underneath-located aluminum plate, and (3) quadrant-based assays [32], scoring the fraction of worms between two low-temperature quadrants and two high-temperature quadrants (heated by infrared bulbs). The main advantage of these assays is their high-throughput nature, because large populations are scored in each plate and the setup can be multiplexed. Some of these assays have been successfully used in candidate-based screens [18] and open-ended genome-scale mutagenesis screens [28]. However, these assays are all endpoint experiments and the obtained scores reflect a complex set of behavioral responses integrated over the duration of the experiment. Qualitative connections between thermal stimulation and individual responses cannot be directly established and the outcome of these assays is more complicated to interpret.

The goal of the present work was to develop a method enabling an efficient assessment of worm thermal sensitivity and facilitating the study of thermal avoidance plasticity mechanisms. We thus faced the challenge of bringing together the main advantages of the above-mentioned methods into a single system that would be able to (1) deliver heat stimuli of adjustable intensity to a whole population of worms on a plate, (2) record and automatically flag heat-evoked reversal responses in a high-throughput manner, and (3) induce thermal adaptation and assess sensitivity changes. We present here the design and main features of this system, as well as the validation of protocols that we developed to assess animal thermal sensitivity and to trigger and quantify thermal adaptation in a high-throughput, quantitative manner. We further reveal that, similar to the impact of persistent noxious heat exposure, repeated stimulations with acute thermal pulses cause a decrease in animal responsiveness. Moreover, by studying the behavior of mutant animals, we show that naive animal thermal sensitivity and the adaptation effects are differentially controlled by CMK-1 and CKK-1. Altogether, our work establishes an efficient method to dissect the molecular mechanisms controlling heat avoidance and its plasticity with *C. elegans*.

## MATERIALS AND METHODS

### Worm strains

The following worm strains were used in this study: DAG800 *cmk-1(pg58) IV*, DAG821 *cmk-1(ok287) IV*, N2, VC691 *ckk-1(ok1033) III*, YT17 *crh-1(tz2) III*.

### Worm preparation for behavioral assays

Adult worms were bleached according to standard protocols and ~150–200 recovered eggs were plated onto individual Nematode Growth Medium (NGM) plates seeded with OP50. Plates were incubated at 20°C for 62–64 h in order to obtain synchronized adults. After incubation,

worms were washed off the plates with distilled water and transferred into 1.5 ml tubes, followed by three washes in order to remove bacterial food. 100–150 worms were transferred onto unseeded NGM plates.

Once transferred, worms were acclimated for 30–60 min before the start of behavioral assays.
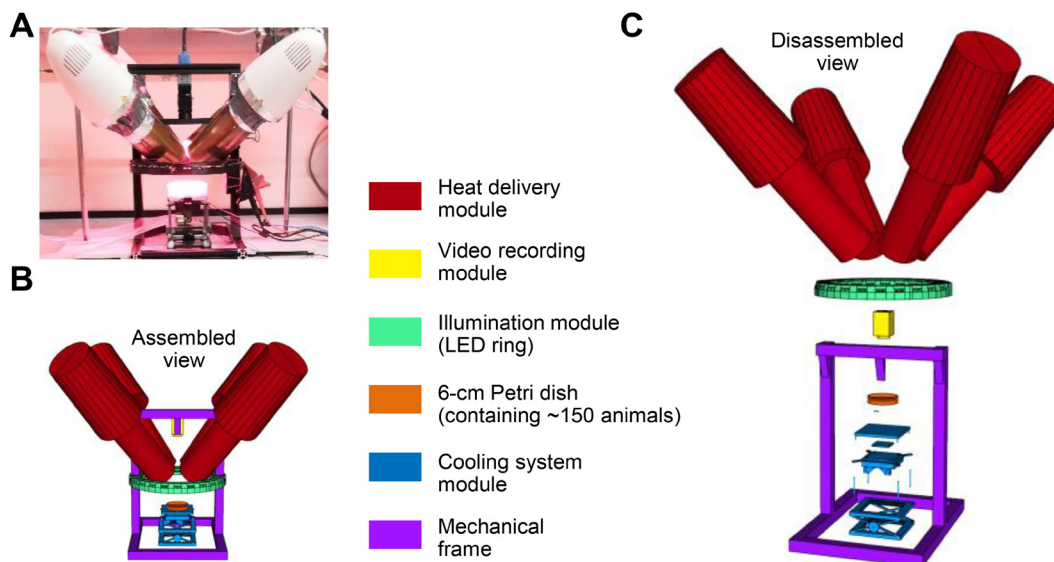


**Figure 1. Overview of the INFERNO hardware. A.** Picture of the INFERNO core system delivering heat. **B.** Front view of a 3D model showing key components of the system in their final assembly configuration. **C.** Exploded-view of the 3D model in (B).

## Design and construction and of the INFERNO hardware

The INFERNO hardware was designed to enable (1) the delivery of acute thermal stimuli of adjustable intensity to a population of worms on a 6 cm NGM plate and (2) the concomitant video recording of worm behavior. An overview of the main hardware components is presented in **Figure 1**. Additionally, **Figure 2** and **Figure 3** provide more detailed descriptions of the functionally distinct modules composing the INFERNO.

*Mechanical frame*: The main support structure (purple structure in **Fig. 1**) was built using V-slot Linear Rail 20 × 20 mm aluminum extrusions and measures 23.5 cm in width, 32.5 cm in length and 34.5 cm in height. The structure joints were connected and reinforced with V-slot-compatible 90° brackets, which were fitted with V-slot-compatible roll-in spring nuts, allowing them to easily slide onto the V-slot Linear Rails. The structure serves as an adjustable rail-mounting system for other components (see module descriptions below).

*Illumination module*: Because an optically opaque heat sink was placed immediately below the specimen Petri dish (see cooling system module description below), worm imaging had to be performed in darkfield and necessitated an oblique illumination. To obtain a homogenous illumination, we designed and 3D-printed a ring structure with 40 slots, each fitting a 5 mm blue LED (Cree, C503B-BCN-CV0Z0461, 3.2 V, 20 mA, 30°, 470 nm). Due to 3D-printer model size limitations, the ring was designed as 4 interlocking quarter-ring segments which assembled into the mountable ring conformation. As illustrated in **Figure 1** and **Figure 3A**, the ring was designed with two diametrically opposed 20 × 20 mm mounting holes, thus fitting onto the lateral vertical V-slot Linear Rail support structures. LEDs were wired as four 10-LED series in parallel and powered with 26 V at 50 mA thanks to a Basetech BT-305 adjustable-voltage DC power supply (**Fig. 3B**). To eliminate LED reflections appearing at the periphery of the agar surface and to reduce background caused by the scattering of light beams hitting the side of the Petri dish, we designed and 3D-printed a cover (**Fig. 3A**), which was placed on top of assay plates before the start of behavioral recordings. Printable 3D models of the ring and cover, named INFERNO_LED_ring_segmented.stl and INFERNO_assay_plate_cover.stl, are available for download (see **GitHub repository** section). Step-by-step instructions to guide the assembly of the device are provided in the Supplementary text sections titled "Background illumination ring: plastic support assembly" and "Background illumination ring: LED circuit assembly" (**Text S1** and **S2**).

*Video recording module*: A DMK 33UX250 camera (The Imaging Source), equipped with a ML-MC25HR macro-zoom lens (Moritex) and an optical filter stack consisting of a FES0500 (Thorlabs), a BG7 and a S8612 (both from Schott) was attached to the upper transversal aluminum rail, such that the camera could hang in between the IR-lamp heating component at a working distance of 18.6 cm from the recorded specimen. The optical filter stack was chosen to block any light produced by the incandescent IR lamps (> 570 nm), while allowing blue light from the LED illumination ring to pass (**Fig. 3C** and **3D**).

*IR-based heat delivery module*: To produce acute heat stimulation over the whole Petri dish surface, four 100 W incandescent infrared lamps (IL-11, 220/230 V, Beurer) were each maintained by an individual stand and aimed towards the Petri dish (**Fig. 1A**). To help accommodate spatial constraints and to prevent radial heat dissipation due to the wide lamp beam angle, the lamps were each fitted with a copper tube (19 cm length, 0.5 mm thickness, 7.25 cm diameter) that reflected IR beams across its interior surface until brought closer to the Petri dish. Copper was chosen due to its high reflectance (> 95% past 600 nm) and cost-efficiency relative to metals with a similarly high reflectance, such as gold and silver. The electronics controlling the IR lamps are schematized in **Figure 2A**. Each lamp was plugged to the mains power

(AC 220/230V) *via* an ENER002 radio-receiver socket (Energenie). Each radio-receiver socket was controlled (timed on/off signals) by executing pre-programmed scripts from a Raspberry Pi (see section

**INFERNO stimulation programs** for script details), which was connected to an ENER314 Pi-mote control board radio-emitter (Energenie) sending socket-specific 433 MHz on/off signals.
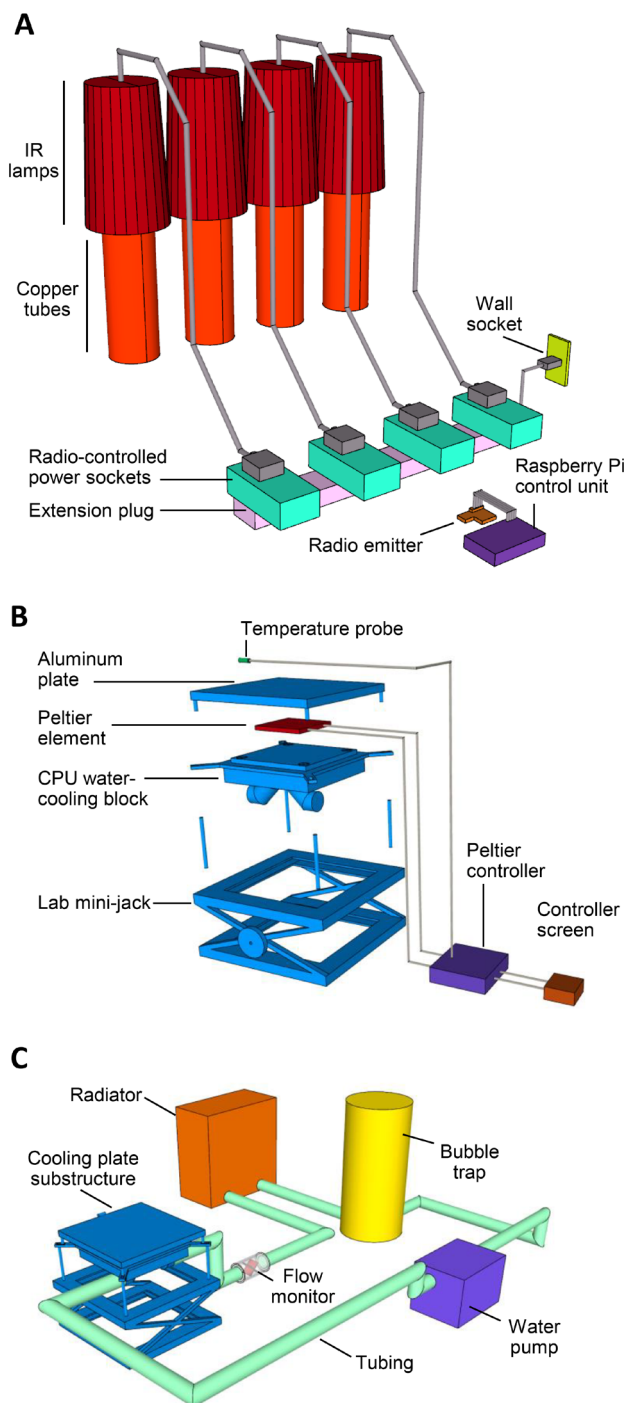


**Figure 2. Overview of the heating and cooling modules of the INFERNO system. A.** Schematic view of the INFERNO heat delivering module showing the electronic component assembly used to program and power the 4 × 100 W infrared lamps. IR lamps are connected to the main AC power supply ("wall socket") *via* radio-controlled power sockets. Each lamp is independently controlled thanks to a Raspberry Pi control unit emitting socket-specific signals to control each of the four lamps individually. **B.** Schematic view of the cooling plate substructure of the INFERNO cooling module showing the assembly of electronics and structural components. The cooling power is continuously adjusted by the Peltier controller using the input from the temperature probe. Heat produced on the hot face of the Peltier element is dissipated *via* a CPU water-cooling block connected to a water-cooling circuit described in (C). **C.** Schematic view of the assembly of water-cooling circuit used to dissipate the heat produced by the Peltier element in the INFERNO cooling system.
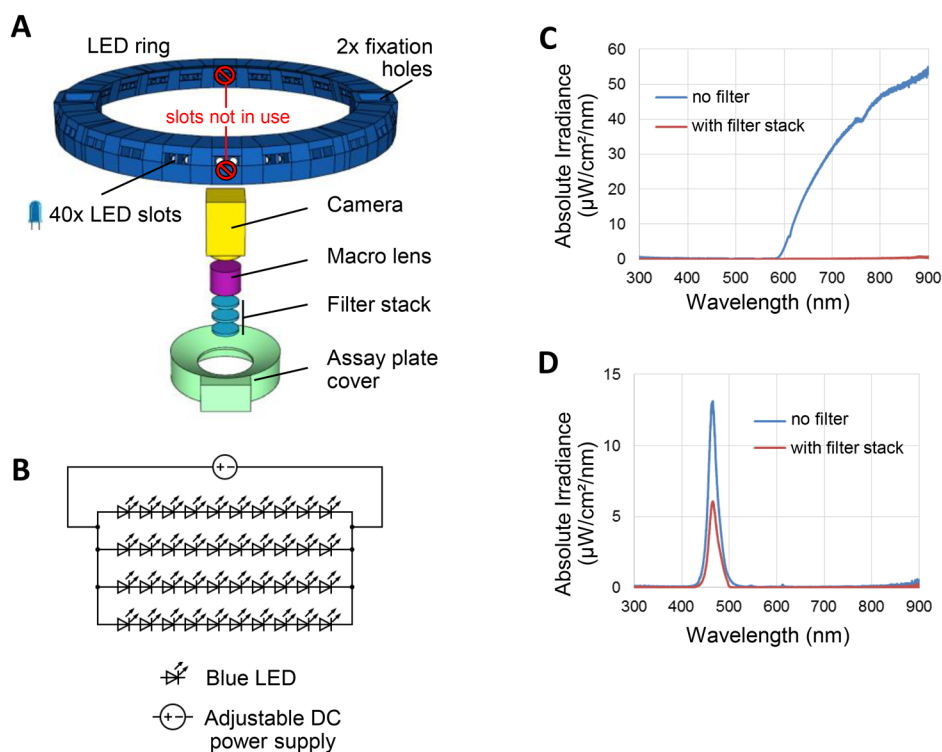
**Figure 3. Description of the video recording and the illumination modules of the INFERNO system. A.** Front view of the 3D rendering of the movie recording system. Stackable components are exploded on the height (z) axis for clarity. **B.** Wiring diagram of the 40× blue LEDs inserted into the blue LED slots in (A). **C** and **D.** Light spectrum emitted by one representative IR lamp (C) or blue LED (D) in the 300–900 nm (corresponding to the camera sensitivity range) and effect of the filter stack. The filter stack completely blocks the contribution of the IR lamps, while allowing a substantial fraction of the blue light to pass.

*Cooling module*: An active water-cooling system was used to cool the plate in between stimuli as fast as possible and to mitigate heat build-up during repeated acute heat stimulations. From top to bottom and as illustrated in **Figure 2B**, the main components of the cooling module were (1) an aluminum plate on which was deposited the Petri dish, (2) a Peltier element, (3) a water circuit-connected CPU cooler to dissipate the heat produced by the Peltier element, and (4) a lab jack used to adjust the height of the cooling module and consequently that of the specimens.

The Peltier element (QC-161-1.6-15.0M) was connected to a Peltier controller (QC-PC-CO-CH1), itself connected to a display (QC-PC-D-CH1) and a temperature probe (NTC 10KΩ) according to the manufacturer instructions (all components from Quickcool). The temperature sensor probe was placed in thermal contact with the assay plate. Separate BT-305 adjustable-voltage DC power supplies were used to power the Peltier element (8 V, max 2.5 A) and the controller and display (each 12.7 V, max 0.1 A). More information about the assembly of the control circuit is given in the Supplementary text section titled "Assembly of the Peltier element temperature control circuit" (**Text S3**). The Peltier element was sandwiched between the aluminum plate (80 × 80 × 3.5 mm) and the CPU cooler (UC-2 LT, Phobya, **Fig. 2B**), each contact surface having first been coated with thermal paste (Arctic Silver 5). A 6 cm long metal support leg was screwed onto the end of each of the four fixation extensions of the CPU cooler. The leg bases were inserted into mounting holes drilled into the top surface of a lab jack (Bochem). The CPU cooler was connected to a heat-dissipating water circuit schematically depicted

in **Figure 2C**. Distilled water was pumped by an Eheim 600 Station II water pump (Alphacool) and flowed through (1) the CPU cooler, (2) a Phobya water-air G-changer 120 radiator, enabling the thermal exchange with surrounding air, (3) a Phobya Balancer 250, serving as a bubble trap and an access for water level adjustment, and (4) a flow indicator (model 71021, Aquatuning) for visual flow verification. For ease of maintenance and quick disassembly, all component input/output ports were fitted with Alphacool Eiszapfen quick release connector kits with G1/4" fittings (model 17282, Aquatuning), with the exception of the CPU cooler, which was fitted with 13/10 mm 90° connectors with G1/4" compression fittings (model 62143, Aquatuning). The connectors were linked together with Clearflex 60 Premium PVC tubing (13 mm external diameter, 10 mm internal diameter, Aquatuning).

## Design and construction of the ThermINATOR hardware

The ThermINATOR hardware was designed to multiplex the delivery of repeated acute heat stimuli on worm populations in NGM plates. An overview of the main hardware components is presented in **Figure 4A** and **4B**.

*IR-based heat delivery module*: Acute heat stimuli were delivered *via* six 175 W incandescent infrared lamps (240 V, Product code 22247, KERBL), each fitted on the supplied E27 power sockets containing a circular mounting slot (1 cm internal diameter). The lamps were slid along a stainless-steel bar (1 cm diameter, 120 cm long) and spaced by 15 cm. The stainless-steel bar was fixed at both ends to a height-adjustable stand (Wolfcraft 3406 stands). For the experimental conditions used

in the present study, the lamp bottom surface was set at 8 cm from the cooled aluminum surface (see subsection below). All lamps were plugged into a 6-socket power extension plug, which was, in turn, plugged to the mains power (AC 220/230V) *via* an ENER002 radio-receiver socket (Energenie). Like for the INFERNO system, stimuli control was achieved by executing a pre-programmed script from a Raspberry Pi (see section **ThermINATOR program** for script details), which was connected to an ENER314 Pi-mote control board radio-emitter (Energenie) sending socket-specific 433 MHz on/off signals.
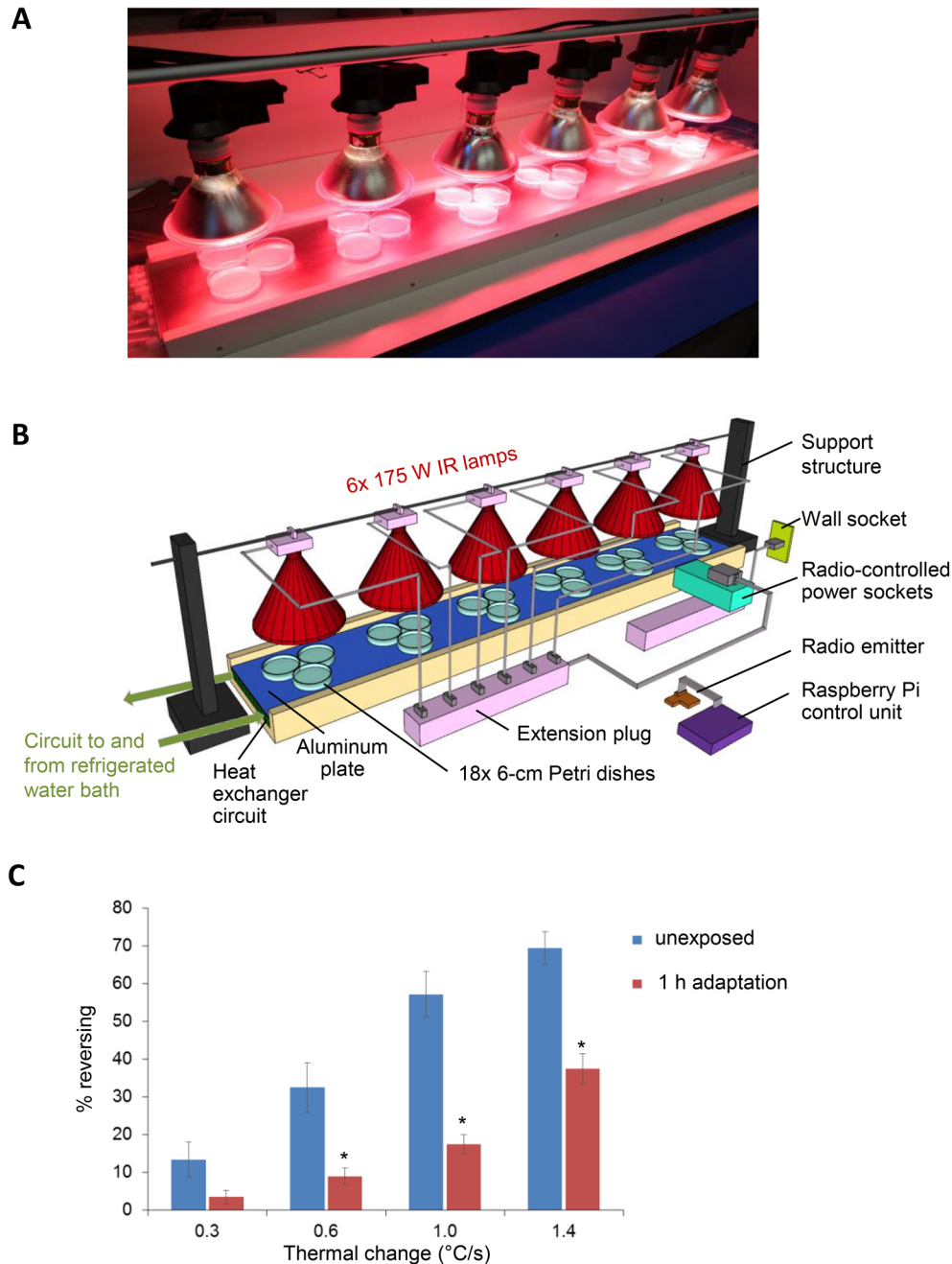


**Figure 4. Detailed structural and behavioral output characterization of the ThermINATOR platform. A.** Picture of the ThermINATOR core system delivering heat. **B.** Perspective view of a 3D rendering model of the ThermINATOR platform describing the main components. The ThermINATOR system enables the repeated stimulation with short heat pulses of multiple (up to 18) worm populations in parallel. **C.** Thermal sensitivity in wild type animals, which had not been exposed to heat prior to the analysis (*unexposed*) or repeatedly stimulated (4 s heat pulses at 0.85°C/s with 20 s ISI) in the ThermINATOR system for one hour (*1 h adaption*). Heat-evoked reversals were quantified with the INFERNO system during a 4 stimulus train at 0.3, 0.6, 1 and 1.4°C/s. Bars are averages (± SEM) of *n* = 8 plates, each containing more than 80 animals.

*Cooling module*: The top surface of the ThermINATOR cooling module, on which NGM Petri dishes were deposited, was a 1000 × 150 × 2 mm aluminum plate. Underneath the plate, a thermal exchanger water circuit was created by aligning ten square-section aluminum tubes (15 × 15 × 1000 mm, wall thickness: 1 mm) side-by-side. Tube fittings were immobilized at the two extremities of each aluminum tube using UHU Patafix and then sealed with Araldite Rapid 2-component epoxy (**Fig. S1B**). Clearflex 60 Premium PVC tubing (10 mm inner diameter, 13 mm outer diameter) was used to connect the aluminum tubes to a Grant LT Ecocool 150 circulating water bath and to each other. The aluminum tubes were connected in series to create a single channel, 10-pass configuration (**Fig. S1C**), thus ensuring homogenous temperature over the whole aluminum plate. The heat exchanger was housed in an insulating structure composed of a Composite/PVC deck board base (150 × 1000 × 24 mm) and MDF side panels (15 × 1000 × 48 mm).

## INFERNO stimulation programs

All scripts listed below can be downloaded from the afferent GitHub repository (see GitHub repository section). These scripts were run from the INFERNO's Raspberry Pi Terminal using the command:

sudo python script_name.py

INFERNO_4stimuli_series.py was run to trigger a temperature stimulation program consisting of: 40 s at baseline temperature, 4 s with 100 W heating (one IR lamp turned on), 20 s of interstimulus interval (ISI), 4 s with 200 W heating (two lamps turned on), 20 s of ISI, 4 s with 300 W heating (three lamps turned on), 20 s of ISI and 4 s with 400 W heating (four lamps turned on).
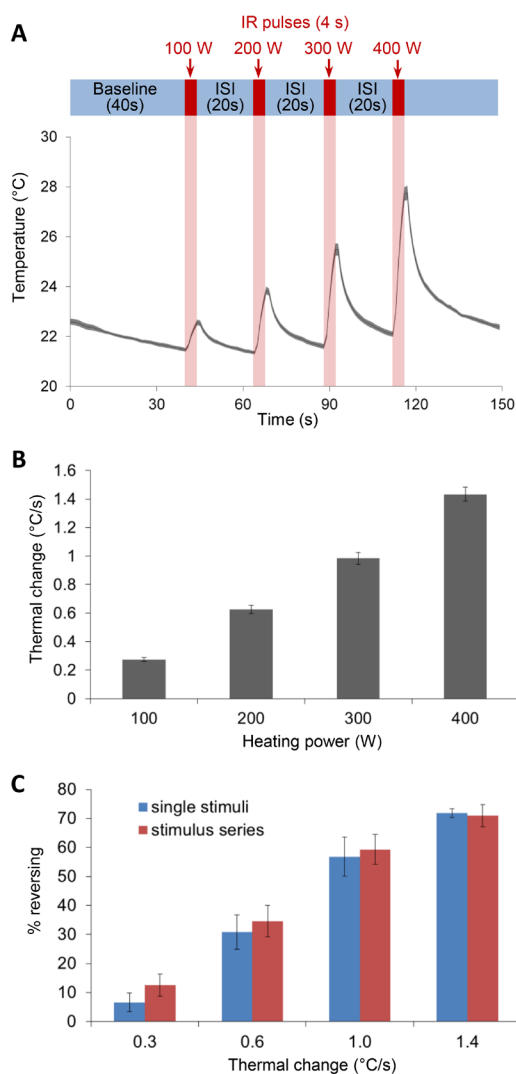


**Figure 5. Heat stimulation and evoked reversal response in the INFERNO system. A.** Short protocol for the thermal sensitivity assessment in the INFERNO system, with the delivery of a series of four heat stimuli of graded intensities (top diagram). Recorded temperature at the surface of NGM plates (bottom plot). Data are depicted as average (black line) ± SEM (grey shade) over 5 different plate recordings. **B.** Calculated average thermal increase during the 4 s stimulation in (A) with bars as average ± SEM. **C.** Heat-evoked reversal analysis in wild type adult animal populations stimulated with the protocol depicted in (A) (stimulus series) as compared to control populations, each stimulated with a single stimulus at the corresponding heat intensities (single stimuli). Bars as average percentage of responding worms ± SEM, from $n ≥ 6$ plates, each recording at least 80 animals. No significant effect revealed by a two-way ANOVA.
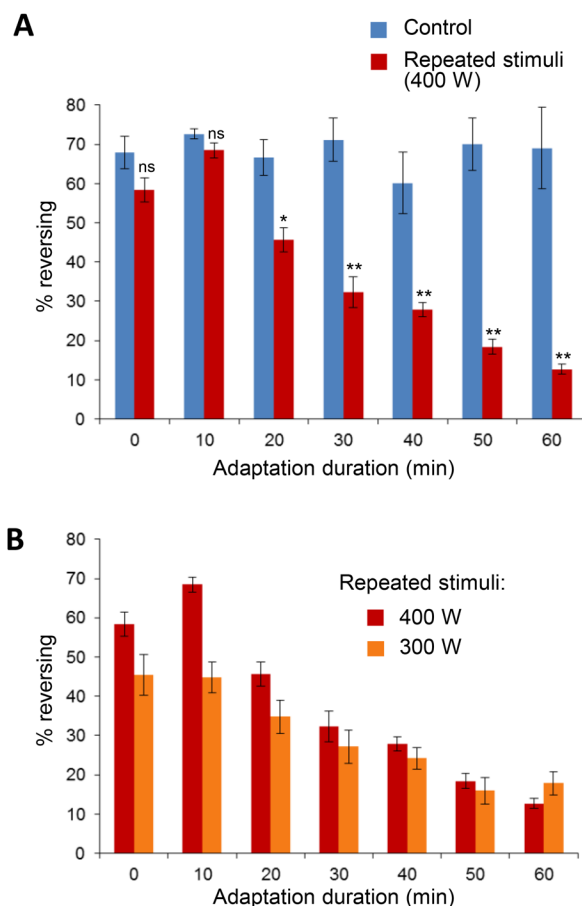
**Figure 6. Adaptation to repeated acute heat stimulations in wild type worms. A.** Fraction of wild type animals reversing in response to 400 W heat pulses, sampled every 10 min during a 1 h period of repeated stimulations (4 s stimuli, 20 s ISI, repeated stimuli) or in the absence of repeated stimulation (control). Bars are averages (± SEM) of $n \geq 3$ plates, each containing more than 80 animals. A two-way ANOVA showed a significant interaction effect between treatment and adaptation duration. ns, not significant; *$P < 0.05$ and **$P < 0.01$ versus control treatment by Turkey post hoc tests. **B.** Comparison of the response adaption to repeated heat stimulations using 400 W or 300 W stimuli. Bars are averages (± SEM) of $n = 5$ plates, each containing more than 80 animals. Thermal profiles corresponding to the repeated stimulation conditions are presented in **Figure S4A** and **S4B**.

INFERNO_1lamp_stimulus.py/INFERNO_2lamp_stimulus.py/INFERNO_3lamp_stimulus.py/INFERNO_4lamp_stimulus.py were run to trigger 4 temperature stimulation programs consisting of 40 s baseline followed by a single 4 s stimulus at 100, 200, 300 or 400 W (with 1, 2, 3, or 4 lamps turned on), respectively. These scripts were used to acquire *single stimuli* data in **Figure 5C**.

INFERNO_adaptation_3lamp.py was run to trigger a temperature program consisting of: 40 s of baseline temperature, followed by an infinite loop of 4 s 300 W stimuli (3 lamps turned on), followed by an ISI of 20 s.

INFERNO_adaptation_4lamp.py was run to trigger a temperature program consisting of: 40 s of baseline temperature, followed by an infinite loop of 4 s 400 W stimuli (4 lamps turned on), followed by an ISI of 20 s.

To generate the adaptation datasets in **Figure 6A** and **6B**, worm plates were treated with either INFERNO_adaptation_3lamp.py or INFERNO_adaptation_4lamp.py at t0 and left to run for 1 h, followed by manual interruption of the script. Alternatively, to generate the control datasets in **Figure 6A**, we ran INFERNO_adaptation_4lamp.py at $t = 0$, $t = 10$, $t = 20$, $t = 30$, $t = 40$, $t = 50$ and $t = 60$ min and left to run for 2:50 min (recording 5 heat pulses), followed by manual interruption of the script. In the case of the control experiments, worm populations were scored only once

at a given time point. Data at $t = 0$, $t = 10$, $t = 20$, $t = 30$, $t = 40$, $t = 50$ and $t = 60$ min thus represent separate batches of unexposed worms.

### ThermINATOR program

The script described below can be downloaded from the afferent GitHub repository (see GitHub repository section). The script was run from the ThermINATOR's Raspberry Pi Terminal using the command:

sudo python ThermINATOR_adaptation.py

ThermINATOR_adaptation.py was run to trigger an infinitely looping temperature program consisting of 4 s of stimulation, with all 6 IR lamps turned on, followed by 20 s ISI with the lamps turned off. The script was manually terminated at the end of the adaptation period.

### Temperature measurements

Temperature at the surface of NGM plates was measured at 1 Hz using a Type K thermocouple connected to a TC-08 Thermocouple Data Logger (Pico Technology) with the PicoLog Recorder software. Temperature measurements were synchronized to start concomitantly with the temperature delivery programs. The tip of the thermocouple was placed in the center of an empty NGM plate, contacting, but not

piercing the surface of the agar.

## Behavioral movie recording using IC Capture

Movies were recorded with IC Capture 2.4 (The Imaging Source) at a 1600 × 1200 pixels resolution, at 8 frames per second, and the resulting .AVI file was encoded as Y800 8-bit monochrome. These parameters were chosen as a tradeoff to limit the size of the movie files, while keeping sufficient spatial and temporal resolution for downstream analysis, and were based on our previous experience with the Multi-Worm Tracker [23]. As recordings using the 4-stimuli train protocol described in **Figure 5** are typically > 2 GB in size, we have provided a cropped and compressed movie for illustration purposes (See **Movie S1**).
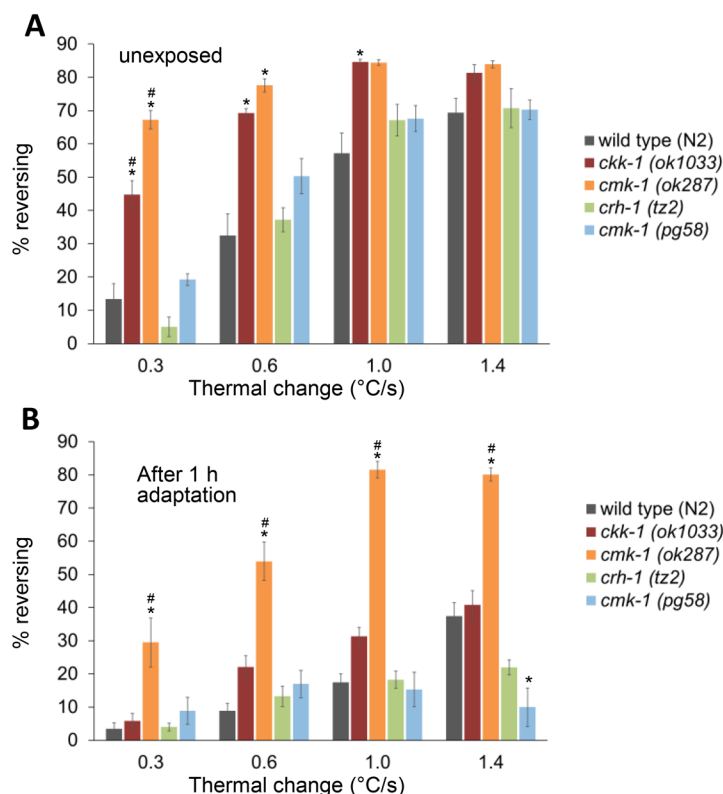


**Figure 7. Heat-evoked response and its plasticity in wild type and mutants for the CKK-1/CMK-1/CRH-1 pathway. A.** Thermal sensitivity in wild type and indicated mutant animals, which had not been exposed to heat prior to the analysis (*unexposed*). Heat-evoked reversals were quantified with the INFERNO system during a 4 stimulus train at 0.3, 0.6, 1 and 1.4°C. **B.** Thermal sensitivity in the same animal populations as in (A), but scored after 1 h of repeated stimulation in the ThermINATOR (4 s heat pulses at 0.85°C/s with 20 s ISI). For both panels, bars are averages (± SEM) of $n \geq 4$ plates, each containing more than 80 animals. For each analysis, two-way ANOVAs showed significant genotype and thermal change main effects as well as significant interaction effects. *$P < 0.01$ versus wild type and #$P < 0.01$ versus all the other mutants by Turkey post hoc tests.

## Multi-Worm Tracker

Movies recorded with IC capture were analyzed using the Multi-Worm Tracker 1.3.0 [33] on a Windows system. We use the configurations detailed below:

*Contrast tab*: Multi-Worm Tracker (MWT) was set to track bright objects. Object Contrast was set to 10%. Fill Hysteresis was set to 50%.

*Size tab*: Image binning was set to 1. Maximum Object Size was set between 150–200 pixels. Minimum object size was set between 80–120 pixels. Object Size Hysteresis was set to 40%.

*Data Output Setting tab*: Skeletonize was turned on. Contour was turned off. Experiment duration was set to the closest multiple of 4 s below the actual recording duration. Auto-start Delay and Raw Image Save Interval were set to 0 s.

*Advanced Settings tab*: Aggregate Output was turned on. Number of Image Adaptation Bands was set to 10. Adaptation Rate was set to 6. Frames of Adaptation was set to 10. Object Border was set to 5.

AFG Resource Name was set to COM1. Bit Depth from Camera was turned on and set to 8. Use Background Division Image Correction was turned off.

## INFERNO reversal flagging pipeline overview

The INFERNO_pipeline_8fps.sh was designed to quantify reversal events of individual worms by interpreting positional data generated by MWT, as well as to automate a number of data pre-processing steps, with built-in batch processing capability. Briefly, reversals were flagged based on the presence of an extremely sharp "turn" taken by the animal (as illustrated in **Fig. S2**), which only occurs when the animal changes its direction of movement (*e.g.*, forward to backward), using the following approach:

(1) Frame by frame xy center of mass coordinates obtained from MWT was converted to a 4-frame moving average. This trajectory smoothing step was implemented to mitigate the impact of the inherent

noise in center of mass definition by the MWT.

(2) For each point of the trajectory (corresponding to frame $i$), the angle change was calculated between two vectors: (a) the vector from coordinates at frame $i - 4$ to coordinates at frame $i$ and (b) the vector from coordinates at frame $i$ to coordinates at frame $i + 4$ (as illustrated in **Fig. S2**).

(3) If the absolute value of the angle change at frame $i$ was greater than 2.4 radians, a reversal event was flagged for that frame.

After the flagging step, behavioral events for individual worm tracks were summarized into 4 s bins, and reported in the output file together with population level data (as illustrated in **Fig. S3**). Heat-evoked reversal response (in **Fig. 4C**, **Fig. 5C**, **Fig. 6** and **Fig. 7**) were calculated from the 4 s bin during which heat was delivered. For a detailed, step-by-step pipeline usage protocol, see the Supplementary text section titled "INFERNO reversal flagging pipeline user guide" (**Text S4**).

### GitHub repository

All scripts and 3D models mentioned within the Materials and Methods section were uploaded to GitHub (https://github.com/ASL-academic/INFERNO-ThermINATOR). Scripts have been annotated with comments (canonically preceded by a '#').

## RESULTS

### Features of the infrared-evoked reversal analysis platform (INFERNO)

In order to analyze thermal avoidance in *C. elegans* in a quantitative and high-throughput manner, we developed a dedicated platform, which we named INFERNO (for infrared-evoked reversal analysis platform). This platform is able to (1) deliver acute thermal stimuli of adjustable intensities to a population of worms, (2) acquire videos of worm behavior, and (3) analyze these videos to quantify reversals. The design and construction of the INFERNO hardware components, as well as the software pipeline used for computer-assisted behavior analysis, is presented in detail in the **Materials and Methods** section. Briefly, and as depicted in **Figure 1**, the INFERNO device includes (1) a Peltier-element based cooling plate on which 6 cm petri dish containing worms are deposited, (2) an LED ring for oblique worm illumination, (3) a macro-zoom and filter-equipped camera for video recording, (4) a set of incandescence IR bulbs for heat delivery, and (5) a control system for the IR bulbs. Our computer analysis behavioral analysis pipeline combined the previously described MWT [33] with custom written python code to flag and count reversal events. With this system, we could monitor and analyze up to ~150 animals in a single experiment in a field of view of 3.5 cm by 2.5 cm and stimulate them with thermal changes up to 1.4°C/s.

### Thermal sensitivity assessment with series of stimuli of graded intensity

Our first objective was to establish and validate a simple and fast protocol to assess animal thermal sensitivity. After a 2 min acclimation period in the recording arena, animals were treated with a train of four heat stimuli of graded intensities: 4 s stimuli at 100, 200, 300, or 400 W with 20 s ISI (**Fig. 5A**). These heat pulses triggered thermal increases at the surface of the plate at 0.3, 0.6, 1.0 and 1.4°C/s, respectively (**Fig. 5B**). We noted a graded increase in heat-evoked reversals reaching ~70% responsiveness

for the strongest stimuli (**Fig. 5C**). To rule out a fast adaptation effect which could occur during the stimuli series, we evaluated a control situation where worm batches naive to heat treatment were exposed to a single heat stimulus at 0.3, 0.6, 1.0 and 1.4°C/s. The reversal induction profile was indistinguishable from that produced by the train of stimuli (compare blue and red bars in **Fig. 5C**), indicating that the thermal intensity-response relationship obtained with the stimulus train protocol is not influenced by an adaptation effect. Collectively, these data indicate that the INFERNO system and the chosen stimulation protocol provide an efficient method to score the thermal sensitivity in a population in less than four minutes.

### Long-term adaptation effect upon repeated acute thermal stimulation

Behavioral plasticity linked to prolonged changes in temperature has been previously studied in *C. elegans* in a variety of contexts, both in the innocuous [29,34,35] and noxious [28,36] range of temperatures. However, nothing is known about the impact of repeated acute thermal stimuli occurring over the hour time range. To investigate this question, we used the INFERNO system to repeatedly stimulate animals during one hour (4 s stimuli, 20 s ISI) and quantify reversal responses. In a first set of experiments, we used the maximal intensity in our system (400 W, 1.4°C/s). Plate surface temperature recordings (**Fig. S4A**) showed a slight general thermal build up during the first 4 min (~10 stimuli), but was stable thereafter. However, the magnitude of the evoked thermal changes was remarkably stable over the full experiment. After 20 min of repeated stimulation, the rate of heat-evoked reversals started to significantly decline, progressively dropping from ~65% to values below 15% after one hour (**Fig. 6A**). This responsiveness decrease may reflect an adaptation to repeated stimulations, the impact of starvation (because worms are maintained on a food-free plate during the experiments), or both. We thus examined control plates with animals that were starved but not exposed to heat, except for a single stimulation at the end of the incubation period during which heat-evoked reversals were measured (no heat control in **Fig. 6A**). We observed no significant reduction in responsiveness during the duration of the experiments in this control situation (**Fig. 6A**). In a second set of experiments, we decreased the stimulation intensity to 1.0°C/s (300 W). We observed a very similar decrease in responsiveness as the one evoked by 1.4°C/s (**Fig. 6B**). Collectively, these data show that repeated heat stimulations produce a robust behavioral adaptation effect.

### Thermal adaptation multiplexed induction platform: ThermINATOR

As described above, the INFERNO system can be used to highlight interesting behavioral plasticity mechanisms. However, data acquisition rate remains relatively limited, because a single adaptation experiment will monopolize the INFERNO system for its whole duration. We therefore created a separate device to induce thermal adaptation in a higher throughput manner, which we named ThermINATOR (for thermal adaptation multiplexed induction platform). A detailed description is available in the Materials and Methods section. Briefly, the ThermINATOR device is composed of (1) a temperature-controlled aluminum plate for heat dissipation on which worm-containing Petri dishes are deposited, (2) a rack of IR bulbs for acute heat stimuli delivery, and (3) a control system for the IR bulbs (**Fig. 4A** and **4B**). The ThermINATOR system can accommodate up to eighteen 6 cm plates or up to

six 10 cm plates, trigger ~1°C/s thermal change at the surface of these plates during stimulation, and dissipate heat in order to return to an innocuous temperature range between the stimuli in 20 ISI stimulation regimes (**Fig. S4C**).

To test the validity of the ThermINATOR system, we used it to induce thermal adaptation in worm populations during one hour, which were then transferred into the INFERNO system to monitor thermal sensitivity using the short 4-stimuli train protocol as an endpoint scoring. We found a significant adaptation effect similar to that induced in the INFERNO system (**Fig. 4C**).

## Specific genetic pathways control thermal sensitivity and adaptation

In order to demonstrate the utility of the ThermINATOR and INFERNO systems to dissect the molecular pathway controlling thermal sensitivity and plasticity, we used them to analyze the behavioral phenotype of mutant animals. We focus on three candidate genes, *cmk-1*, *ckk-1*, and *crh-1*, which are part of the same canonical pathway [37] and which had been previously implicated in behavioral plasticity evoked by constant temperature changes [27]. Nothing is known however on whether and how they could modulate behavioral response to repeated acute thermal stimuli.

First, we assessed thermal sensitivity in naive, unstimulated animals. We found that the loss of *ckk-1* or *cmk-1*, in *ckk-1(ok1033)* and *cmk-1(ok287)* mutants respectively, increased baseline animal sensitivity with a significantly left-shifted heat-response curve (**Fig. 7A**). In contrast, sensitivity in naive animals was unaltered in mutants carrying a *cmk-1* gain-of-function allele *(pg58)* or in *crh-1* loss-of-function animals *(crh-1(tz2))*. These data suggest that the activity of the two upstream kinases in the CKK-1/CMK-1/CRH-1 pathway negatively regulates baseline thermal sensitivity, while the potential downstream effector CRH-1 is not required.

Second, we evaluated the impact of one hour of repeated stimulations in the same mutants. The thermal sensitivity in the in *cmk-1(ok287)* loss of function mutant was markedly higher than in wild type, but, conversely, slightly reduced in the *cmk-1(pg58)* gain-of-function mutant (**Fig. 7B**). These results are in line with previous observations made with noxious heat thermogradient assays [28]. In contrast, loss of *ckk-1* or *crh-1* produced no significant impact.

Collectively, these results suggest that (1) CMK-1 signaling is required to lower thermal sensitivity in naive, unexposed animals as well as upon adaptation to repeated stimuli, (2) CKK-1 is required only in unexposed animals, and (3) CRH-1 plays no major role in either situation. The thermal sensitivity level in unexposed or adapted animals is thus controlled by genetically separable molecular pathways.

## DISCUSSION

Here, we introduce and successfully validate two new platforms that will facilitate the analysis of thermal avoidance and associated plasticity in *C. elegans*.

The INFERNO system, which allows the scoring of up to ~150 animals in a single experiment, combines the high-throughput nature of a population-based assay with the ability to analyze acute stimulus-locked behavioral events. With the short protocol presented here, which uses a series of 4 stimuli of graded intensities, a snapshot of the overall sensitivity of a large worm population can be obtained in just

a few minutes. In combination with the ThermINATOR system, it is possible to evaluate the adaptation effects caused by repeated stimulations. Here, as a proof-of-utility for the platforms, we analyzed the behavior in wild type and a few candidate mutants to assess their thermal sensitivity in naive and adapted states. In the future, the approach will allow for larger-scale genetic screens, as well as deeper cellular and circuit analyses, which have all already been initiated in our laboratory.

One of our goals in developing these platforms was to make them readily accessible to other laboratories, both in terms of cost and ease of construction/use. For example, we chose to integrate unmodified heating lamps directly available from general public stores and implemented radio-controlled sockets to mitigate any electrical safety concerns that may exist with high-voltage (220/230 V) appliances. Another important aspect is the platform modularity, which makes them readily evolvable and adaptable to specific needs. During the development of the INFERNO system, we made specific design choices to meet our specific goals in terms of stimuli intensity, heat dissipation, data acquisition/analysis rate, and behavioral information content. If a higher content behavioral analysis is desired, one could, for example, increase the camera resolution, decrease the size of the field of view and/or use another type of Multiworm tracker, such as the recently developed Tierpsy tracker [38,39]. These modifications may result in an increase of the computing load, storage requirements, data analysis time and/or a decrease in the number of animals analyzed in a single experiment. Another example of modification could be to replace the presented Peltier-based cooling module by a refrigerated circulating water bath. This choice would significantly raise the cost of the instrument, but could, in principle, provide similar heat dissipation efficacy and simplify the assembly of the system.

Our data show that wild type worms reduce their heat-evoked reversal responses when repeatedly exposed to noxious heat. The effect is already visible after 20 min and continues to progressively decline until one hour. In principle, this response decrease could reflect a sensory adaptation process in the pathway coupling heat and reversals, a general fatigue effect, or the result of thermal damage. We favor the first model because the response in *cmk-1(ok287)* mutants stimulated for one hour was as strong as that in untreated wild type animals (**Fig. 7A** and **7B**). Many questions are now open about this sensory adaptation process, in particular on the influence of the ISI duration (as shown for mechanical stimulation [40]), on the reversibility of the phenomenon and on the molecular and cellular mechanisms involved. Although future work using the INFERNO and ThermINATOR systems will allow detailed investigations on these questions, we already started to characterize the molecular pathways underpinning this plasticity and tested the impact of mutations in genes encoding proteins working in the CKK-1/CMK-1/CRH-1 pathway. This pathway was chosen because we and others had previously demonstrated its implication in the plasticity induced by long-lasting thermal changes [28,29], in the salt learning process [30] and in response to repeated acute mechanical stimulations [31]. Our data confirm that CMK-1 can act to increase thermal sensitivity. We show that the loss of *cmk-1* has a more pervasive impact than that of *ckk-1*. This observation could be explained by the fact that *ckk-1* is expressed in a narrower subset of neurons than *cmk-1*. It is also possible that CKK-1 activation of CMK-1 is selectively required to lower baseline sensitivity in unexposed animals, but not to modulate adaptation.

In conclusion, our work describes a productive methodology for the high-throughput analysis of thermal avoidance in *C. elegans* and

its plasticity. Combined with the powerful genetic tools available in *C. elegans* for the comprehensive analysis of molecular and cellular processes controlling neural functions, our method will accelerate the discovery of potentially conserved modulatory mechanisms.

## Author contributions

Conceptualization, Methodology, Formal Analysis, Writing—Original Draft, Writing—Review & Editing: D.A.G. and A.-S.L. Investigation, Resources: A.-S.L. Supervision, Funding Acquisition: D.A.G.

## References

1. Burrell BD (2017) Comparative biology of pain: What invertebrates can tell us about how nociception works. J Neurophysiol 117: 1461-1473. doi: 10.1152/jn.00600.2016. PMID: 28053241

2. Walters ET (2018) Nociceptive Biology of Molluscs and Arthropods: Evolutionary Clues About Functions and Mechanisms Potentially Related to Pain. Front Physiol 9: 1049. doi: 10.3389/fphys.2018.01049. PMID: 30123137

3. St John Smith E (2018) Advances in understanding nociception and neuropathic pain. Journal of Neurology 265: 231-8. doi: 10.1007/s00415-017-8641-6. PMID: 29032407

4. Gregory NS, Harris AL, Robinson CR, Dougherty PM, Fuchs PN, et al. (2013) An overview of animal models of pain: disease models and outcome measures. J Pain 14: 1255-1269. doi: 10.1016/j.jpain.2013.06.008. PMID: 24035349

5. D'Amour FE, Smith DL (1941) A method for determining loss of pain sensation. J Pharmacol Exp Ther 72: 74-9.

6. O' Callaghan JP, Holtzman SG (1975) Quantification of the analgesic activity of narcotic antagonists by a modified hot-plate procedure. J Pharmacol Exp Ther 192: 497-505. PMID: 1168252

7. Woolfe G, Macdonald AD (1944) The evaluation of the analgesic action of Pethidine hydrochloride (Demerol). J Pharmacol Exp Ther 80: 300-7.

8. Hargreaves K, Dubner R, Brown F, Flores C, Joris J (1988) A new and sensitive method for measuring thermal nociception in cutaneous hyperalgesia. Pain 32: 77-88. doi: 10.1016/0304-3959(88)90026-7. PMID: 3340425

9. Gold MS, Gebhart GF (2010) Nociceptor sensitization in pain pathogenesis. Nat Med 16: 1248-1257. doi: 10.1038/nm.2235. PMID: 20948530

10. Dubin AE, Patapoutian A (2010) Nociceptors: the sensors of the pain pathway. J Clin Invest 120: 3760-3772. doi: 10.1172/JCI42843. PMID: 21041958

11. Im SH, Galko MJ (2011) Pokes, sunburn, and hot sauce: Drosophila as an emerging model for the biology of nociception. Dev Dyn 241: 16-26. doi: 10.1002/dvdy.22737. PMID: 21932321

12. Tobin DM, Bargmann CI (2004) Invertebrate nociception: behaviors, neurons and molecules. J Neurobiol 61: 161-174. doi: 10.1002/neu.20082. PMID: 15362159

13. Komuniecki R, Harris G, Hapiak V, Wragg R, Bamber B (2011) Monoamines activate neuropeptide signaling cascades to modulate nociception in C. elegans: a useful model for the modulation of chronic pain?. Invert Neurosci 12: 53-61. doi: 10.1007/s10158-011-0127-0. PMID: 22143253

14. White JG, Southgate E, Thomson JN, Brenner S (1986) The structure of the nervous system of the nematode Caenorhabditis elegans. Philos Trans R Soc Lond B Biol Sci 314: 1-340. doi: 10.1098/rstb.1986.0056. PMID: 22462104

15. Corsi AK, Wightman B, Chalfie M (2015) A Transparent Window into Biology: A Primer on Caenorhabditis elegans. Genetics 200: 387-407. doi: 10.1534/genetics.115.176099. PMID: 26088431

16. Hobert O (2003) Behavioral plasticity in C. elegans: paradigms, circuits, genes. J Neurobiol 54: 203-23. doi: 10.1002/neu.10168. PMID: 12486705

17. Wittenburg N, Baumeister R (1999) Thermal avoidance in Caenorhabditis elegans: an approach to the study of nociception. Proc Natl Acad Sci U S A 96: 10477-10482. doi: 10.1073/pnas.96.18.10477. PMID: 10468634

18. Glauser DA, Chen WC, Agin R, Macinnis BL, Hellman AB, et al. (2011) Heat avoidance is regulated by transient receptor potential (TRP) channels and a neuropeptide signaling pathway in Caenorhabditis elegans. Genetics 188: 91-103. doi: 10.1534/genetics.111.127100. PMID: 21368276

19. Oakes MD, Law WJ, Clark T, Bamber BA, Komuniecki R (2017) Cannabinoids activate monoaminergic signaling to modulate key C. elegans behaviors. J Neurosci 37: 2859-2869. doi: 10.1523/JNEUROSCI.3151-16.2017. PMID: 28188220

20. Oakes M, Law WJ, Komuniecki R (2019) Cannabinoids stimulate the TRP channel-dependent release of both serotonin and dopamine to modulate behavior in C. elegans. J Neurosci 39:4142-52. doi: 10.1523/jneurosci.2371-18.2019. PMID: 30886012

21. Leung K, Mohammadi A, Ryu WS, Nemenman I (2016) Stereotypical escape behavior in Caenorhabditis elegans allows quantification of effective heat stimulus level. PLoS Comput Biol 12: e1005262. doi: 10.1371/journal.pcbi.1005262. PMID: 28027302

22. Nieto-Fernandez F, Andrieux S, Idrees S, Bagnall C, Pryor SC, et al. (2010) The effect of opioids and their antagonists on the nocifensive response of Caenorhabditis elegans to noxious thermal stimuli. Invert Neurosci 9: 195-200. doi: 10.1007/s10158-010-0099-5. PMID: 20397037

23. Schild LC, Glauser DA (2013) Dynamic switching between escape and avoidance regimes reduces Caenorhabditis elegans exposure to noxious heat. Nat Commun 4: 2198. doi: 10.1038/ncomms3198. PMID: 23887613

24. Glauser DA (2014) How and why Caenorhabditis elegans uses distinct escape and avoidance regimes to minimize exposure to noxious heat. Worm 2: e27285. doi: 10.4161/worm.27285. PMID: 24744986

25. Mohammadi A, Byrne Rodgers J, Kotera I, Ryu WS (2013) Behavioral response of Caenorhabditis elegans to localized thermal stimuli. BMC Neurosci 14: 66. doi: 10.1186/1471-2202-14-66. PMID: 23822173

26. Ghosh R, Mohammadi A, Kruglyak L, Ryu WS (2012) Multiparameter behavioral profiling reveals distinct thermal response regimes in Caenorhabditis elegans. BMC Biol 10: 85. doi: 10.1186/1741-7007-10-85. PMID: 23114012

27. Glauser DA, Goodman MB (2016) Molecules empowering animals to sense and respond to temperature in changing environments. Curr Opin Neurobiol 41: 92-98. doi: 10.1016/j.conb.2016.09.006. PMID: 27657982

28. Schild LC, Zbinden L, Bell HW, Yu YV, Sengupta P, et al. (2014) The balance between cytoplasmic and nuclear CaM kinase-1 signaling controls the operating range of noxious heat avoidance. Neuron 84: 983-996. doi: 10.1016/j.neuron.2014.10.039. PMID: 25467982

29. Yu YV, Bell HW, Glauser D, Van Hooser SD, Goodman MB, et al. (2014) CaMKI-dependent regulation of sensory gene expression mediates experience-dependent plasticity in the operating range of a thermosensory neuron. Neuron 84: 919-926. doi: 10.1016/j.neuron.2014.10.046. PMID: 25467978

30. Lim JP, Fehlauer H, Das A, Saro G, Glauser DA, et al. (2018) Loss of CaMKI Function Disrupts Salt Aversive Learning in C. elegans. J Neurosci 38: 6114-6129. doi: 10.1523/JNEUROSCI.1611-17.2018. PMID: 29875264

31. Ardiel EL, McDiarmid TA, Timbers TA, Lee KCY, Safaei J, et al. (2018) Insights into the roles of CMK-1 and OGT-1 in interstimulus interval-dependent habituation in Caenorhabditis elegans. Proc Biol Sci 285: 20182084. doi: 10.1098/rspb.2018.2084. PMID: 30429311

32. Nkambeu B, Salem JB, Leonelli S, Marashi FA, Beaudry F (2018) EGL-3 and EGL-21 are required to trigger nocifensive response of Caenorhabditis elegans to noxious heat. Neuropeptides 73: 41-48. doi: 10.1016/j.npep.2018.11.002. PMID: 30454862

33. Swierczek NA, Giles AC, Rankin CH, Kerr RA (2011) High-throughput behavioral analysis in C. elegans. Nat Methods 8: 592-598. doi: 10.1038/nmeth.1625. PMID: 21642964

34. Goodman MB, Sengupta P (2017) The extraordinary AFD thermosensor of

C. elegans. Pflugers Arch 470: 839-849. doi: 10.1007/s00424-017-2089-5. PMID: 29218454

35. Kimata T, Sasakura H, Ohnishi N, Nishio N, Mori I (2012) Thermotaxis of C. elegans as a model for temperature perception, neural information processing and neural plasticity. Worm 1: 31-41. doi: 10.4161/worm.19504. PMID: 24058821

36. Kotera I, Tran NA, Fu D, Kim JH, Byrne Rodgers J, et al. (2016) Pan-neuronal screening in Caenorhabditis elegans reveals asymmetric dynamics of AWC neurons is critical for thermal avoidance behavior. Elife 5: doi: 10.7554/eLife.19021. PMID: 27849153

37. Kimura Y, Corcoran EE, Eto K, Gengyo-Ando K, Muramatsu M, et al. (2002) A CaMK cascade activates CRE-mediated transcription in neurons of Caenorhabditis elegans. EMBO Rep 3: 962-966. doi: 10.1093/embo-reports/kvf191. PMID: 12231504

38. Javer A, Currie M, Lee CW, Hokanson J, Li K, et al. (2018) An open-source platform for analyzing and sharing worm-behavior data. Nat Methods 15: 645-646. doi: 10.1038/s41592-018-0112-1. PMID: 30171234

39. Javer A, Ripoll-Sánchez L, Brown AEX (2018) Powerful and interpretable behavioural features for quantitative phenotyping of Caenorhabditis elegans. Philos Trans R Soc Lond B Biol Sci 373: 20170375. doi: 10.1098/rstb.2017.0375. PMID: 30201839

40. Ardiel EL, Rankin CH. An elegant mind: Learning and memory in Caenorhabditis elegans. Learn Mem 17: 191-201. doi: 10.1101/lm.960510.

## Supplementary information

**Text S1**. Background illumination ring: plastic support assembly.

**Text S2**. Background illumination ring: LED circuit assembly.

**Text S3**. Assembly of the Peltier element temperature control circuit.

**Text S4**. INFERNO reversal flagging pipeline user guide.

**Figure S1**. Details of the ThermINATOR cooling module heat exchanger.

**Figure S2**. Illustration of the INFERNO reversal flagging criterion.

**Figure S3**. Illustration and explanation of the INFERNO output file.

**Figure S4**. Thermal profiles during adaptation protocols with the INFERNO and ThermINATOR systems.

**Figure S5**. Visual assembly guide for the blue light illumination ring.

**Figure S6**. Visual assembly guide for the blue light LED circuit.

**Movie S1**. Sample recording using the INFERNO system.

Supplementary information of this article can be found online at http://www.jbmethods.org/jbm/rt/suppFiles/324.